SPE 130768

Multi-Field Asset Integrated Optimization Benchmark

Silvya Dewi Rahmawati, SPE, NTNU; Curtis Hays Whitson, SPE, NTNU/PERA; Bjarne Foss, SPE, NTNU; and Arif Kuntadi, SPE, NTNU

This paper was prepared for presentation at the SPE EUROPEC/EAGE Annual Conference and Exhibition held in Barcelona, Spain, 14–17 June 2010.

Abstract

Integrated modeling of multi-field assets, from subsurface to market, is challenging due to the complexity of the problem. This paper is an extension of the SPE 121252, model based integration and optimization gas cycling benchmark [Juell, et al., 2009], extending two gas-condensate fields to two full-field multi-well models. Additionally, a full-field model is added to the Juell benchmark, introducing an oil field undergoing miscible WAG injection, where most data are taken from the SPE 5 Reservoir Simulation Comparative Project. All reservoir models are compositional, but using different EOS representations. A base case scenario is defined with fixed numbers and locations of producers and injectors.

A common field-wide surface processing facility is modeled with emphasis on water handling, NGL extraction, sales-gas spec, and gas reinjection. The surface process model interacts with the three reservoir models through two main mechanisms – (1) water- and gas-handling constraints, and (2) distribution of available produced gas for reinjection into the three reservoirs.

The field asset model provides long-term production forecasts of gas, oil, and NGL revenue. Cost functions are introduced for all major control variables (number of wells, surface facility selection and operating conditions, injection gas composition). Net present value is used as the target objective function.

This paper will evaluate optimal production strategies for the base case benchmark problem, using several key control variables and field operational constraints. Optimization performance will be tested with a few solver algorithms. The benchmark will be provided to the industry through application data files, network infrastructure, and results from our integrated optimization model.

Introduction

Operation of complex assets may require a holistic view of the value chain. This is particularly important if the different parts of the value chain are tightly connected. Present industrial practice typically takes a silo approach in the sense that one part of the supply chain is treated quite separate from other parts. This is pronounced in the upstream area where for instance a decision support application for optimally allocating well production may include well and pipeline models. The downstream boundary condition is typically a constant pressure at the inlet separator. Similarly an optimizer for the surface process does not include models of the upstream system. This implies that the inlet separator acts as a “dividing wall” between two optimizers even though the two subsystems might be tightly connected. An example of this is when the gas output from the surface facility is fed back into the upstream system through gas-lift wells or gas injectors. There are many reasons for the silo-like situation. Different parts of the supply chain recruit people with different backgrounds and they use quite different decision support tools. This limits integration even in situations where integration has an obvious potential.

Several researchers have conducted research on various integration topics. [Bailey et al., 2005] and [Cullick et al., 2003] discussed complex petroleum field projects applying uncertainty analysis, but the surface process facility was not considered. [Nazarian, 2002] integrated ECLIPSE® and HYSYS® simulators to calculate integrated field operation in a deepwater oil field.

Those simulators were coupled by using Automation and Parallel Virtual Machine and applying a genetic algorithm for the optimization. [Hepguler & Barua, 1997] and [Hepguler et al., 1997] discussed an integrated application for reservoir-production strategies and field development management. In this case, the ECLIPSE reservoir simulator was coupled with the surface and production network simulator and the optimizer (Netopt). Run time can be a challenge in integrated application, especially when closely linked high-fidelity models are tightly connected. [Barroux et al., 2000] proposed a practical solution to reduce run time of the coupled simulators. [Trick, 1998] applied a somewhat different procedure from [Hepguler et al., 1997], using the same interface. In this case an ECLIPSE black oil reservoir simulator was coupled to a surface gas deliverability forecasting model, FORGAS. The use of integrated optimization in a day-to-day operations setting of the LNG value chain was studied by [Foss and Halvorsen, 2009)]. To reduce computation time they chose simple models for all system components. A sizable gain could be identified by integrating all models into one decision support application as opposed to dividing them into two applications; one for the upstream part and the other for the LNG plant. [Tomasgard et al., 2007] presents a natural gas value chain model and integration applying an upstream perspective and a stochastic portfolio optimization.

The literature citings above identifies a potential for integrating models in decision support tools. Moreover, integrated simulation and optimization is clearly regarded as an interesting but challenging topic. Hence, in this paper we present a benchmark problem which is designed to assess the potential of an integrated approach in decision support tools. A realistic benchmark as well as a base case will be defined in the following sections. Further, a sensitivity analysis of key decision variables will be presented in addition to some early optimization results. The paper ends with some conclusions and directions for further work.

Integrated Model

The model presented in this paper is rich and complex enough to represent the value chain from reservoir to export and thus suitable as a benchmark for integrated operations and optimization (I-OPT). The upstream part of the I-OPT model includes two gas-condensate reservoirs and an oil reservoir while the surface process system includes gas and liquid separation as well as an NGL plant. The model also includes an economic component as indicated in Fig. 1. All model components have been designed using realistic assumptions and parameter values. Further, the project is designed with close links between the upstream and downstream parts of the model, partly due to gas re-injection. This is important since the I-OPT model is designed to study and assess the business value of integrated optimization as a decision support method. Integrated optimization in this context is defined as applications which utilize several different models along the value chain, for instance a reservoir model and a surface process model, in *one* optimization-based application as opposed to two separate applications for the reservoir and surface part, respectively. Hence, the I-OPT model is designed to challenge the conventional silo approach. The I-OPT model is further designed to study decisions both on a life-cycle horizon as well as shorter time frames. The surface facility model is a steady-state model while the reservoirs are modeled using dynamic models to account for depletion effects. The model is an extension of the full-field model from a previous paper [Juell, et al., 2009].

The I-OPT model will be presented in the following sections. Complete documentation of the I-OPT model including the base case discussed later will also be made available.

Reservoir Description

The reservoir models include two gas-condensate reservoirs and an oil reservoir. The gas-condensate reservoirs are scaled up from [Juell, et al., 2009] and the oil reservoir is a scaled up version of a miscible WAG project [Killough and Kossack, 1987]. In the base case each reservoir is producing through 5 production wells and injection operations are conducted through 8 injection wells which perform gas injection wells in the gas-condensate reservoirs and WAG injection in the oil reservoir. The production and injection wells are perforated through all layers. The well locations for each reservoir are shown in Fig. 2(b) and are given in Table 10.

The gas-condensate reservoir models consist of $36 \times 36 \times 4$ grid blocks and the oil reservoir $35 \times 35 \times 3$ grid blocks. The horizontal permeability distributions for the three reservoirs vary from a low value in the south west region towards higher permeability values in the north east. This is shown for one layer in Fig. 2(a). The permeability distribution range is presented on Table 1. There are two faults in the horizontal direction, one is non-communicating and the other is partially communicating. The non-communicating fault separates low permeability and medium permeability areas. The partially communicating fault separates the medium and high permeability areas. The non-communicating shale in the vertical direction occurs between layers 3 and 4 in

the lean gas-condensate reservoir, between layers 1 and 2 in the rich gas-condensate reservoir and between layers 2 and 3 in the oil reservoir. The reservoir models are compositional. The composition for the gas-condensate reservoirs consist of 9 components and the composition for the oil reservoir consists of 6 components. The initial fluid composition for the gas–condensate reservoirs are referred to [Juell, et al., 2009] and for the oil reservoir is presented in Table 7 to Table 9. The compositional reservoir models are run using the SENSOR® reservoir simulator.

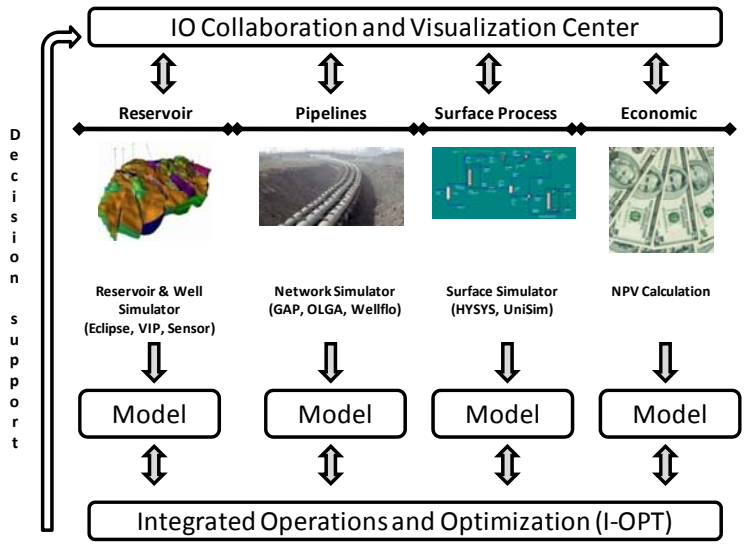

Fig. 1 – Integrated optimization schematic.

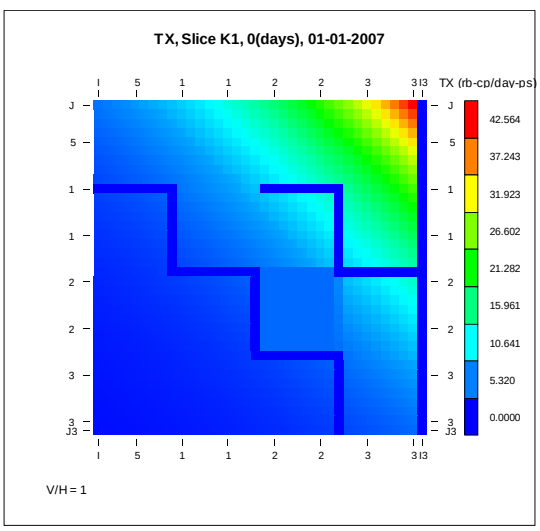

(a) Transmissibility distribution for lean gas-condensate reservoir in first layer.

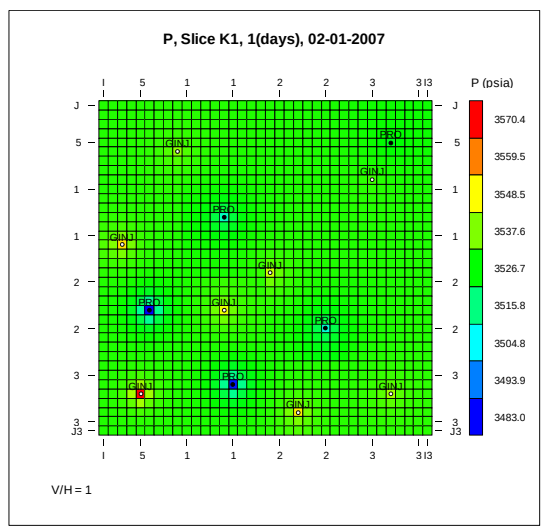

(b) Production and injection well placement for the lean gas-condensate reservoir.

Fig. 2 – Reservoir description of heterogeneity and well placement.

PVT Description

Compositional reservoir modeling usually offers better accuracy than black oil reservoir modeling, but in many cases a black oil model is still preferred due to shorter computation time. Therefore, Black Oil Tables (BOT) are supplied as an alternative to the EOS PVT models. BOT is generated by Constant Compositional Expansion (CCE) experiment for the same surface process used in the reservoir model. PhazeComp® is used to conduct the PVT simulations. Fig. 3 shows the key black-oil properties:

B_o, μ_o, R_s, R_v for the lean gas-condensate, rich gas-condensate and oil reservoirs. The rich gas-condensate reservoir has different initial fluid composition as a function of depth; therefore, 4 different BOTs are shown for this reservoir.

Table 1 – Horizontal permeability and thickness distributions.

Layer	Permeability (md)			Thickness (m)	
	Lean Gas Condensate	Rich Gas Condensate	Oil	Gas Condensate Reservoir	Oil Reservoir
1	13-1300	35-3500	50-5000	9.1	6.1
2	4-400	4.5-450	5-500	9.1	9.1
3	2-200	2.5-250	20-2000	15.2	15.2
4	15-1500	1-100	x	15.2	x

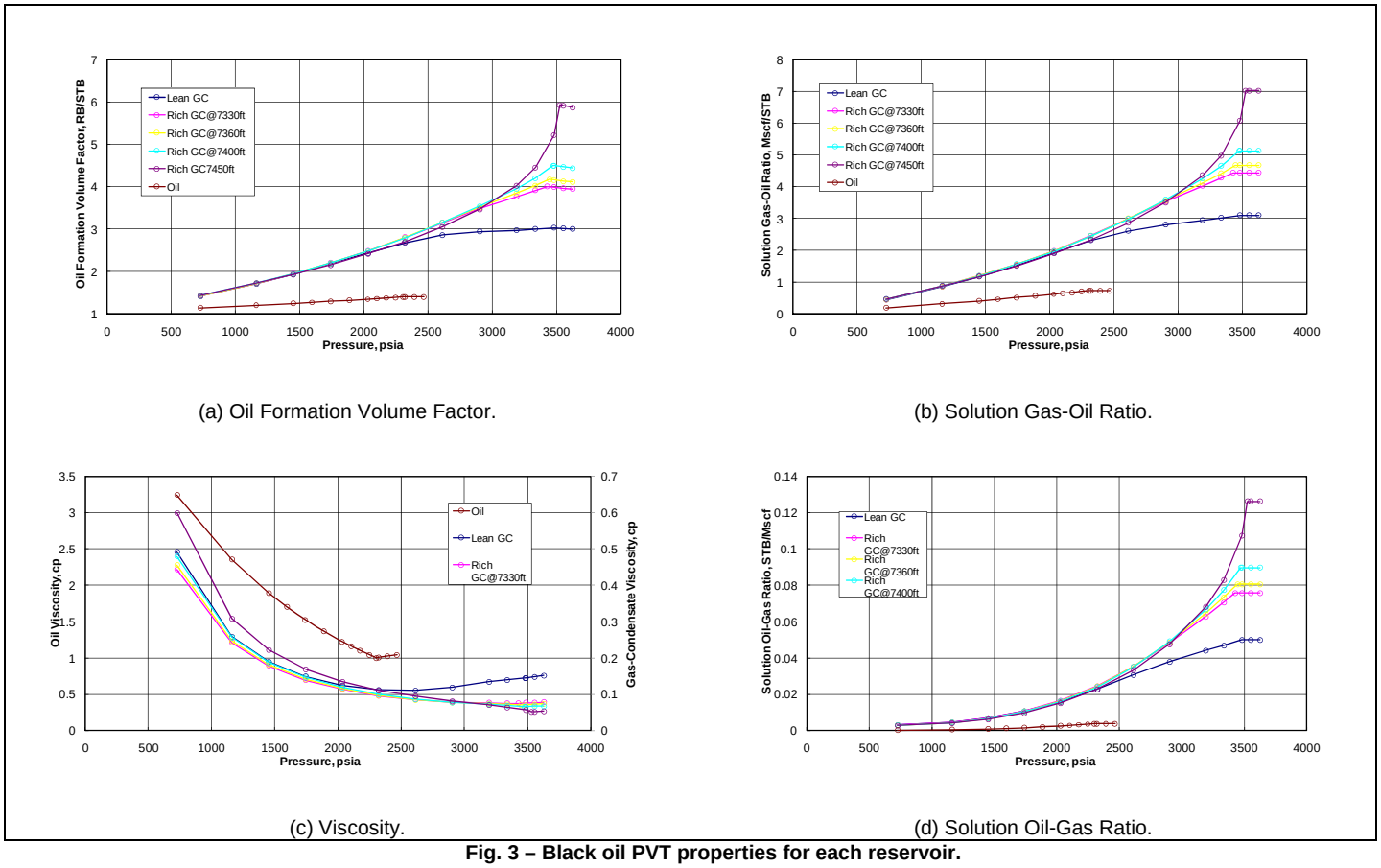

(a) Oil Formation Volume Factor.

(b) Solution Gas-Oil Ratio.

(c) Viscosity.

(d) Solution Oil-Gas Ratio.

Fig. 3 – Black oil PVT properties for each reservoir.

Well Vertical Flow Models

The vertical well flow model is integrated into the reservoir simulator by introducing the Tubing Head Pressure table (THP table). The THP table for each well is generated using the PROSPER® simulator and a single THP table is provided for each reservoir. The data range and underlying model that are used to generate the THP table are provided in Table 2. The application of the reservoir simulator to the well-reservoir system produces a tabulation of bottom-hole pressure versus surface rate, phase surface rate ratios, and tubinghead pressure. The data in the THP table reflects a particular PVT characterization, tubing size, length,

roughness and geometric configuration. Bilinear interpolation is used to determine bottom-hole pressure for given values of rate, GOR (GLR, LGR), water cut or WOR and THP [Sensor Reference Manual, 2009]. The producer rate constraint, the injector maximum bottom-hole pressure constraint and the plateau rate target are presented in Table 3. During a simulation, the minimum tubing head pressure (THP) for each production well becomes a constraint. The THP for each well is compared with the manifold pressure from the surface calculation and is redefined as THP. The reason for this is to change the minimum THP to equal the manifold pressure when the manifold pressure is greater than the THP.

Table 2 – Initial data for generating tubing tables.

Parameter	Reservoir		
	Lean GC	Rich GC	Oil
Rate (Units)	Mscf/D	Mscf/D	STB/D
Min:(Intervals):Max	100:(20):50000	100: (20):50000	100:(20):25000
OGR	STB/MMscf	STB/MMscf	GOR (scf/STB)
	5:(10):600	5:(10):600	300:(10):10000
WGR	STB/MMscf	STB/MMscf	w ater cut (STB/STB)
	0	0	0:(10):1
THP	psia	psia	psia
	100:(10):3550	100:(10):2500	100:(10):5000
Pressure drop correlation	Gray	Gray	Hagedorn & Brow n

Table 3 – Well and field constraints.

Reservoir	Producer rate constraint (std m^3/D)	Minimum Producer THP constraint (bara)	Maximum Injector BHP constraint (bara)	Plateau rate target (m^3/D)
Lean Gas Condensate	5.4 E+05	68.95	275.8	27 E+05
Rich Gas Condensate	5.4 E+05	68.95	275.8	27 E+05
Oil	1920	68.95	310.3	9600

Surface Pipeline Flow Models

HYSYS is used to calculate the pressure loss in the pipeline. The pressure drop in pipelines is solved through backward calculation; however, enough information must be supplied to complete the material and energy balance calculations. The solution procedure starts at the outlet, i.e. as a pressure in the inlet separator, where the pressure is known, and at the inlet where the temperature and rate are known. HYSYS then performs a backward calculation to find the inlet pressure. There are two pipelines transporting gas and one transporting liquid, as shown in Fig. 4. The inlet pressure at the gas pipe is calculated using the Weymouth equation [Ikoku, 1984] and the pressure drop at the liquid pipe (oil and water) is calculated by using the Beggs and Brill correlation [Beggs and Brill, 1973]. Heat transfer in the ground is assumed to be steady state and the same material is assumed in all pipes. The gas pipe is assumed to be isothermal and the liquid pipe non-isothermal. The pipeline data is presented in Table 4.

Surface Process Description

The surface model is a steady state model where input streams will vary with time since these inputs are determined by the reservoir models. The surface process model is implemented in HYSYS. The surface process model is separated into two main separation processes, liquid and gas separation. The liquid separation process consists of multi-stage separation processes. Separators 1 and 4 are three-phase separation processes which separates gas, oil and water. Separators 2 and 3 are two-phase separation processes which separates gas and liquid. In sequence, the pressure for each separator is 56.2 bara, 21.7 bara, 4.5 bara and 1.01 bara. Further, there is a second-step drying stage for each separator to extract more liquid from the separated gas stream.

The final product from the liquid separation process is condensate. A water pump is installed to transfer water to the water disposal facility.

The gas separation process consists of CO_2 removal, H_2O removal and continues to the NGL plant; each process is simplified by representing it by a splitter model. In the real field separation process, complex unit operations are required such as distillation columns in a NGL plant. The Dew Point Controller (DPC) unit is installed to produce high NGL recovery. There are six final products from the gas separation process facility. These are sales gas, fuel gas, reinjected gas to the lean gas-condensate reservoir, reinjected gas to the rich gas-condensate reservoir, reinjected gas to the oil reservoir and NGL. There are two products from the NGL plant, NGL vapor and NGL liquid. NGL vapor mainly consists of methane, ethane and propane and will be reinjected to the oil reservoir while NGL liquid mainly consists of heavy components which will be sold as NGL. The surface process plant architecture is presented in Fig. 4.

Table 4 – Surface pipeline data.

Parameter	Unit	Reservoir		
		Lean GC	Rich GC	Oil
Length	km	5	10	11.5
ID	in	10	10	12
Roughness	mm	4.60E-02	4.60E-02	4.60E-02
Pressure Drop Correlation	-	Weymouth	Weymouth	Beggs and Brill

Thermodynamic Models

Peng-Robinson 1979 (PR-1979) was used as the EOS model in the HYSYS, PROSPER and SENSOR simulators. A check was made on the consistency of all PVT calculations. PhazeComp as a PVT simulator was used to generate PVT information and compared with HYSYS. The only difference in EOS input parameters was the volume shift factors where HYSYS (incorrectly) requires the negative of the actual value.

Economic Model

The goal of the integrated model is to study the potential of integrated optimization. Hence, an economic model is developed to calculate the asset value. The model is based on Net Present Value (NPV), Eq.1. NPV is calculated in a normal manner by introducing a discount factor. The operational expenses (OPEX), however, are in the base case defined by a fixed amount. The OPEX covers the pipeline and well operational costs and it is estimated around 1 million USD per day for the base case. The field revenue is obtained from gas, NGL and condensate sales. The daily cost is summed from the volume of water production and injection, CO_2 removal and power consumption. For the base case the initial condensate and NGL prices are 503 USD/m^3 (80 USD/bbl), the initial gas price is 0.21 USD/m^3 (6 USD/Mcf), the initial water production and injection cost is 18.4 USD/m^3 (2.93 USD/bbl), the initial CO_2 removal cost is 15.4 USD/MT, and the initial power cost is 5 cents/kWh. NPV is calculated as shown below. The project time step $\Delta t_p(t)$ is 1 year and $N = 20$ in the base case. Hence, the total simulation time is 20 years.

$$J_{NPV} = \sum_{t=1}^{N} \left[\frac{q_g(t)r_g(t) + q_c(t)r_c(t) + q_{NGL}(t)r_{NGL}(t) + \left(q_{wi}(t) + q_{wp}(t)\right) r_w(t) + p(t)r_p(t) + M_{CO_2}(t)r_{CO_2}(t)}{(1+d)^t} - OPEX(t) \right] \Delta t_p(t) \quad (1)$$

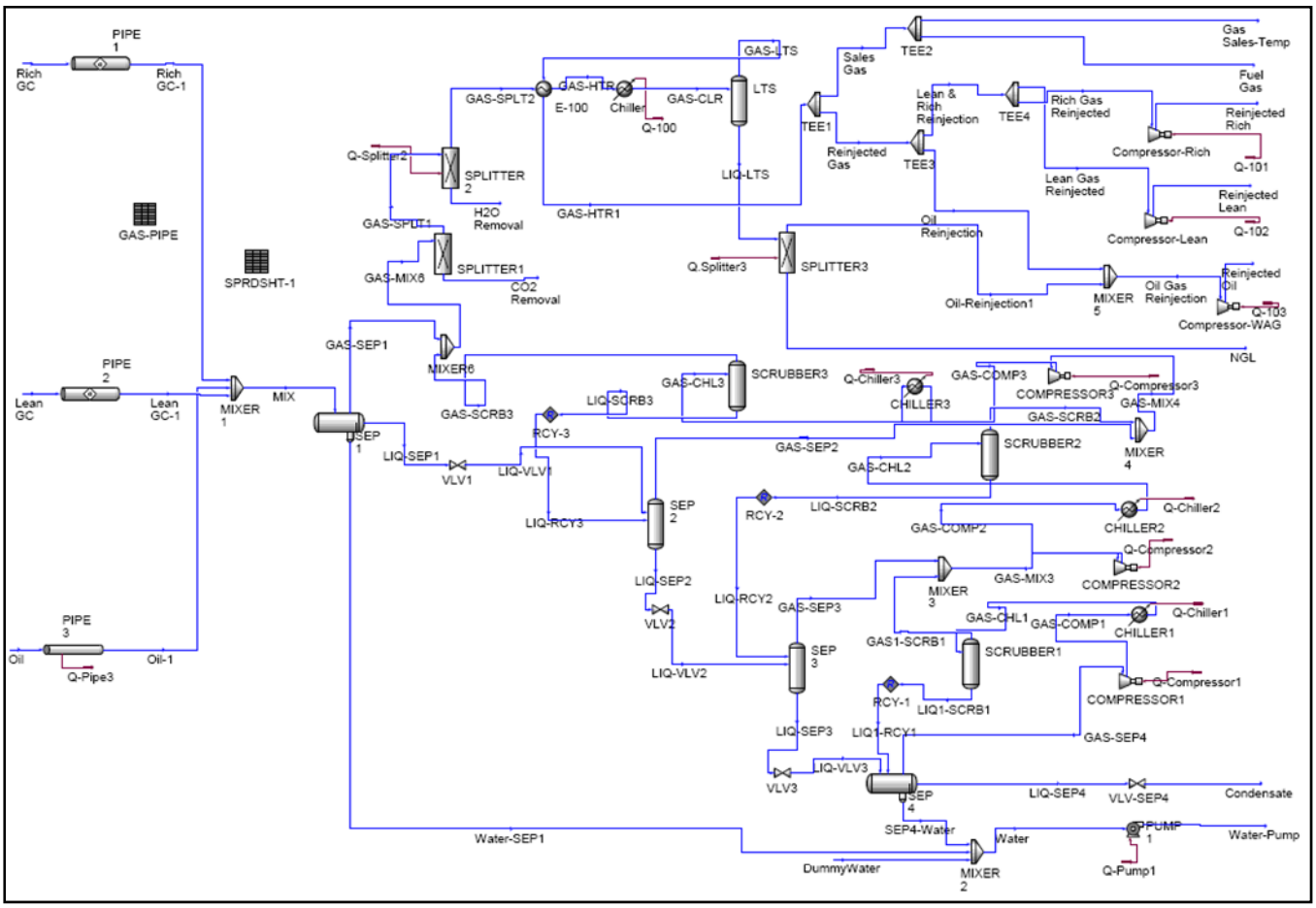

Fig. 4 – Surface process facility schematic.

Software Applications and Model Integration

As already mentioned the reservoir and well models are simulated with SENSOR and the well vertical flow models were substituted inside the reservoir simulator by entering THP tables generated by PROSPER. The gathering manifold, pipeline and surface process facility are simulated using HYSYS. Pipe-It® is used as the integration platform for the I-OPT model meaning that it integrates and schedules the different applications for a given project run. This is similar to the solution in [Juell et al., 2009].

The I-OPT model is run by linking all software applications that transfer data from one application to another providing dynamic communication between the reservoir-well-manifold-pipeline and surface process facility simulators. The HYSYS application is accessed through Automation and is written in the object-oriented programming language Ruby. HYSYS supports several integration techniques since it is Object Linking and Embedding (OLE) compliant.

The hydrocarbon molar flow rates and molar water rate from each reservoir are transferred to the surface simulator. These data are modified through Ruby to create the equivalent input for HYSYS. HYSYS simulates the surface facility and returns the injection compositions and injection rates to the reservoir simulator through Pipe-It. The production rates, power consumption and mass of CO_2 removal are transferred to the economic model. The compositional problem translation from the reservoir to the surface facility is solved by mixing all components from the gas-condensate reservoirs and the oil reservoir. The total number of components in the surface facility is 16, with 9 components from the gas-condensate reservoirs and 6 components from the oil reservoir. Water is also treated as a component. In this paper, the lumping and de-lumping processes are not considered but a subsequent study will compare black-oil reservoir simulation using BO-to-compositional conversions. Complete documentation will be provided such that the benchmark can be implemented on alternative platforms. For example, the SENSOR reservoir simulator may be replaced by an ECLIPSE simulator; HYSYS may be replaced by UniSim®, etc.

Base Case Description

Some base case data have already been introduced. Further base case data are shown in Table 5. The total simulation time is 20 years and injection is active during the first 10 years. The simulation scenario starts with injection for 10 years, followed by depletion of the gas-condensate reservoirs, and water injection for the oil reservoir. The base case WAG scenario is based on scenario 2, SPE 5 Comparative solution project [Killough and Kossack, 1987]. The gas injection rate is 566336 m^3/D (20000 Mcf/D), the water injection rate, 7154 m^3/D (45000 bbl/D) and the change from water to gas injection and vice verse occurs every 91.25 days[1]. For the oil reservoir there are two active constraints, a gas oil ratio constraint (1781 Sm^3/m^3 or 10 Mcf/STB) and a watercut constraint (0.83). A well will shut in if it reaches one of these constraints, and re-opened one year later. It may be noted that the water supplied for the water injection comes from an external source; hence, it is not directly linked to the process facility.

The numerical solution method works as follows. The static facility model is solved once every project time step which in the base case is 1 year. The computed gas injection rates are then supplied to the reservoir simulator which is run for 1 year. The average values during the project time step are input parameters to the static process model which is solved. During each project time step, the amount of injected gas into the oil reservoir need not equal the available gas calculated by the surface facility simulator. If the available gas is less than the injected gas, then the additional gas should be purchased and it will become an additional cost. On the contrary, if the available gas is greater than the injected gas, then the rest will be sold and hence generate added revenue. The annual NPV performance for the base case is presented in Fig. 5. This figure shows for the base case parameters, the field should be operated for 10 years, from an economic point of view. The smaller project time step gives a more-accurate NPV is also shown in the figure.

Table 5 – Base case parameters.

Variable	Value
Sales Gas fraction	0.4
Fuel Gas fraction	0.3
Gas-Condensate Reinjection fraction	0.6
Lean Reinjection fraction	0.5
DPC Temperature (C)	-30
Discount Factor (%)	10
Injection Time (days)	3650
Project Time Step (days)	365
Total Simulation Time (days)	7300

Sensitivity Analysis

The base case simulator and scenario will now be analyzed by perturbing some key parameters. Fig. 6 shows the sales gas, NGL, condensate, water injection and gas injection for the base case. This figure shows that sales gas increase after the end of injection scenario. Parameter analysis is conducted for key decision variables in this benchmark case. These include:

- The dew point temperature controlling NGL extraction.
- The gas sales fraction (fraction sales gas of total produced gas, TEE1 top-right in Fig. 4).
- The gas-condensate reinjection fraction (fraction of reinjected gas into gas condensate reservoirs, TEE3 top-right in Fig. 4)
- The lean reinjection fraction (fraction reinjected gas into lean reservoir, TEE4 top-right in Fig. 4).

[1] The SENSOR WAG logic specifies injection rates and cumulative slug volume per cycle.

For the reservoir aspect, it is possible to optimize the WAG period and the amount of gas and water injection rates. All decision variables are left constant during a simulation run.

Figs. 7 – 11 show single parameter analysis for each optimization variables and Figs. 12 – 14 show surface parameter analysis. During the simulation, the field-operation will be terminated if the field revenue could not pay the operational expenses. Figs. 7 – 14 show the day at which a maximum NPV is reached. It can be concluded from the study that the model is highly nonlinear and there may be local optima. A robust optimization method is needed to find the global optimum for this model. Fig. 15 shows surface parameter analysis for NPV versus injection end time and simulation end time. Fig. 16 shows the NPV as a function of different project time step for the base case. The simulation was run on a 2.67 GHz, 2 Quad core CPU with 8 GB of RAM. Applying a project time step of 365 days (1 year) and the run time was about ~336 seconds.

Fig.16 shows that there is only a small gain to be made in terms of run time if the project time step is increased beyond 1 year. However, a shorter project time step increases the computations substantially. NPV is shown for the varying project time steps and it tends to converge towards a value. The cumulative NPV change with project time step is shown in Fig. 5, where it is seen that the annual NPV is consistently underestimated for increasing project time steps. One might argue for different project time steps depending on the run time and hardware resources available. [Juell, et al., 2009] improved the NPV result for a given project time step size by introducing intermediate "division" project time steps whereby reservoir results were fed to the (fast, approximate) process model, without feedback. This approach was not used in our benchmark because the surface process CPU time was much higher, and contributed a significant part of the total project run time.

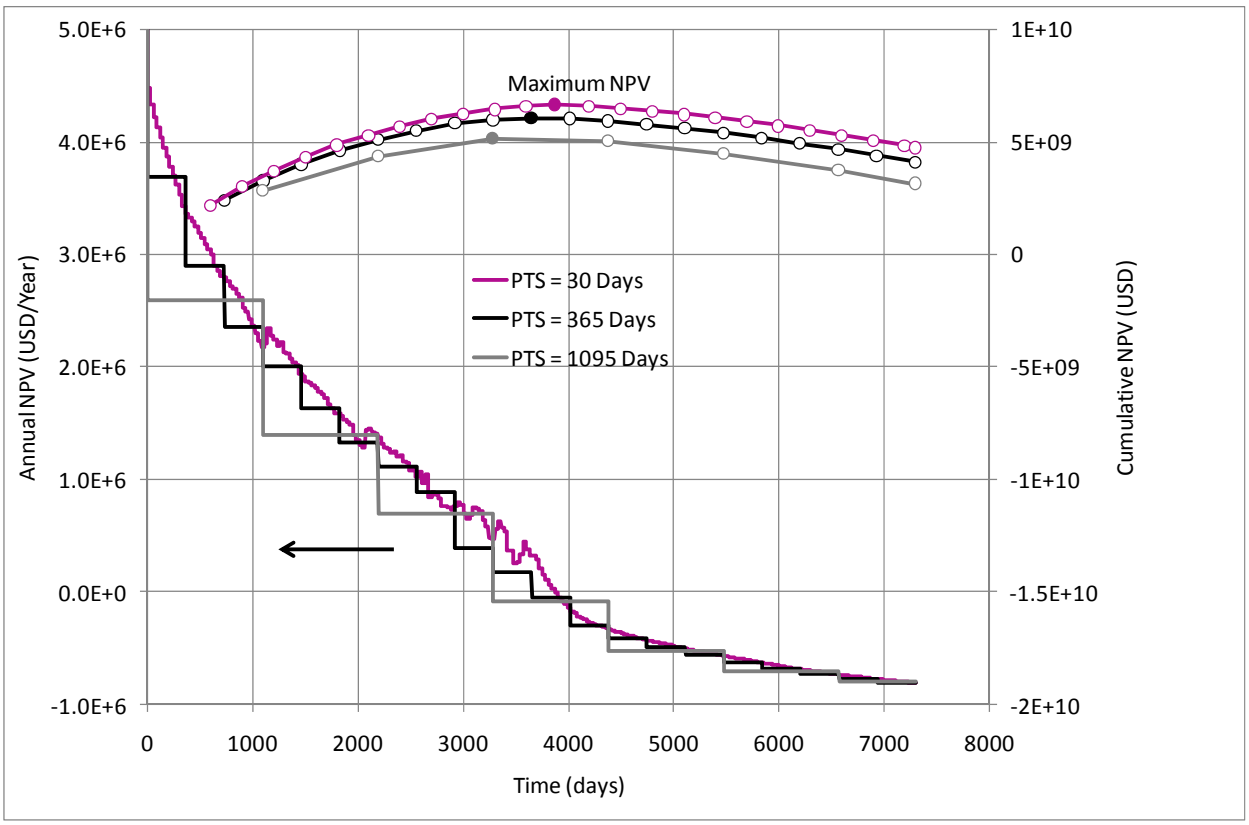

Fig. 5 – NPV variation with time.

Optimization

The optimization is conducted by implementing the Nelder and Mead (1965) reflection simplex algorithm, modified to handle constraints and variable bounds. This algorithm is a popular direct search method especially for nonlinear problem [Lagarias, et al., 1998] where derivatives are not available or reliable. The method is applied for two different optimization scenarios to maximize the NPV. The decision variables for the first scenario are DPC temperature, sales gas fraction, gas-condensate reinjection fraction

and lean gas-condensate reinjection fraction. The decision variables for the second scenario are sales gas fraction, DPC temperature, gas injection rate and water injection rate for WAG scenario and WAG period. The first scenario focused on the surface facilities parameter optimization, while the second scenario is the combination of surface facilities and reservoir parameters. These optimization models can be described as the following:

Scenario 1

$$\max_{\{f_{sg}, f_{R_{gc}}, f_{R_L}, T_{DPC}\}} J_{NPV}$$

with the following constraints on the decision variables

$$0.1 \le f_{sg} \le 0.9, \qquad 0.1 \le f_{R_{gc}} \le 0.9, \qquad 0.1 \le f_{R_L} \le 0.9, \qquad -55 \le T_{DPC} \le -10$$

Scenario 2

$$\max_{\{f_{sg}, T_{DPC}, q_{gi_O}, q_{wi}, \Delta t_{WAG}\}} J_{NPV}$$

with the following constraints on the decision variables

$$0.1 \le f_{sg} \le 0.9, \qquad 55 \le T_{DPC} \le -10, \qquad 0 \le q_{gi_O} \le 1.81E+06, \qquad 0 \le q_{wi} \le 8744.30, \qquad 30 \le \Delta t_{WAG} \le 365$$

The base case value is used as the initial value for the optimization. The optimization results for scenario 1 are: $f_{sg} = 0.1, f_{R_{gc}} = 0.38, f_{R_L} = 0.67, T_{DPC} = -41.2^oC$ and the optimization results for scenario 2 are: $f_{sg} = 0.16, T_{DPC} = -34.8^oC$, $\Delta t_{WAG} = 42.51$ days, $q_{gi} = 1.81E+06$ $\mathrm{m^3/D}$, $q_{wi} = 7613$ $\mathrm{m^3/D}$. The comparison between base case and the optimization results is presented in Table 6 and early shows the potential of optimization since NPV has increased ~9% and ~15%, respectively. Scenario 1 requests 267 number of iterations for converging on the optimum solutions, while scenario 2 requests 334 iterations. The base case CPU run time for optimization scenario 1 is 28.11 hours and for optimization scenario 2 is 34.45 hours.

The CPU run time for a single I-OPT case increases dramatically for smaller $\Delta t_p(t)$, as seen in Fig. 16. Also, the maximum NPV is a strong function of $\Delta t_p(t)$ because of numerical integration error (see Fig. 5). However, Fig. 16 clearly shows that the magnitude of total NPV error is more-or-less constant for a given $\Delta t_p(t)$, with the slope of maximum NPV versus project time step being approximately constant – as seen in Fig. 16 for the base case and the optimum cases found from scenarios 1 and 2. We therefore assume that the surface of maximum NPV is insensitive to $\Delta t_p(t)$, and compromise using a $\Delta t_p(t)$ of 1 year for optimizations. Once an optimal case is located, the I-OPT project is rerun with a smaller project time step (e.g. 1 month) to obtain a more-accurate "true" value of maximum NPV.

Conclusions

The presented I-OPT model is suitable for assessing the potential of integrated optimization since the upstream and downstream parts of the model are tightly coupled. The field asset model provides long-term production forecasts of gas, oil, and NGL revenue. All aspects of the model are realistic and well suited for both life-cycle analysis and shorter time-frame studies. The model is implemented in state-of-the-art software. Detailed documentation is made available so that alternative software platforms with the necessary functionality may be used to study the same muti-field, integrated asset. The base case run time for the presented implementation on a standard laptop computer is ~6 mins. Optimization has a clear potential since the multi-variable scenarios considered in this paper reveal an NPV increase of 10% - 15% compared to the base case gas injection scenario, and 25% or more improved NPV compared with conventional gas depletion/water-injection oil recovery strategy. The absolute NPV value depends on the project time step used, but not the NPV surface topology which determines the location of optimal field operation.

Recommendations for Further Work

The benchmark will be used as a platform for a variety of analyses. One obvious option is to compare the potential of an integrated optimization approach to a silo approach where the upstream and downstream parts of the system are optimized separately. Further, different types of decision variables may be explored, for instance alternative drilling programs like the number and location of wells. The use of closed-loop approaches like Model Predictive Control as a means to improve an open-loop approach can also be of interest.

Nomenclature

B_O	=	Oil FVF, RB/STB
d	=	Discount factor
f_{sg}	=	Sales gas fraction
f_R	=	Reinjected gas fraction, $f_R = 1 - f_{sg}$
$f_{R_{gc}}$	=	Gas-condensate reinjection fraction
f_{R_O}	=	Oil reinjection fraction, $f_{R_O} = 1 - f_{R_{gc}}$
f_{R_L}	=	Lean gas-condensate reinjection fraction
f_{R_R}	=	Rich gas-condensate reinjection fraction, $f_{R_R} = 1 - f_{R_L}$
GOR	=	Gas Oil Ratio, scf/STB
GLR	=	Gas Liquid Ratio, STB/MMscf
N	=	Total project time step
M_{CO_2}	=	Mass of CO_2 removal, MT/day
q_c	=	Surface condensate production rate, m^3/day
q_g	=	Surface gas sales, m^3/day
q_{gi}	=	Gas injection rate, m^3/day
q_{NGL}	=	Surface NGL production rate, m^3/day
q_{wi}	=	Water injection rate, m^3/day
q_{wp}	=	Surface water production rate, m^3/day
r_c	=	Condensate price, USD/ m^3
r_{NGL}	=	NGL price, USD/ m^3
r_p	=	Power cost, USD/kWh
r_w	=	Water injection and production cost, USD/ m^3
r_{CO_2}	=	CO_2 removal cost, USD/MT
R_s	=	Solution gas-oil ratio, Mscf/STB
R_v	=	Solution oil-gas ratio, STB/Mscf
T_{DPC}	=	Dew Point Controller temperature, ^oC
WOR	=	Water Oil Ratio, STB/STB
WGR	=	Water Gas Ratio, STB/MMscf

Greek Symbols

$\Delta t_p(t)$	=	Project time step, days
Δt_{WAG}	=	WAG cycle time, days
μ	=	Viscosity, cp
ρ	=	Density, kg/m^3

References

1. Juell, A., Whitson, C.H., and Hoda, M.F. 2009. Model Based Integration and Optimization Gas Cycling Benchmark. Paper SPE 121252 presented at the SPE EUROPEC/EAGE Conference, 8-11 Juni 2009, Amsterdam, The Netherlands.
2. Bailey, W.J., Couet, B., and Wilkinson, D. 2005. Framework for Field Optimization to Maximize Asset Value. SPE 87026-PA. SPE Reservoir

Engineering Journal 8(1): 7-21.
3. Cullick, A.S., Heath, D., Narayanan, K., April, J., and Kelly, J. 2003. Optimizing Multiple-Field Scheduling and Production Strategy with Reduced Risk. Paper SPE 84239 presented at the 2003 SPE Annual Technical Conference and Exhibition, 5-8 October 2003, Denver, Colorado.
4. Nazarian, B. 2002. Integrated Field Modeling. Ph.D. Thesis, The Norwegian University of Science and Technology (NTNU), Norway.
5. Hepguler, G., and Barua, S. 1997. Integration of A Field Surface and Production Network With A Reservoir Simulator. SPE 38937-PA. SPE Computer Applications Journal.
6. Hepguler, G., Dutta-Roy, K., and Bard, W.A. 1997. Applications of A Field Surface & Production Network Simulator Integrated With A Reservoir Simulator. SPE 38007-MS presented at SPE Reservoir Simulation Symposium, 8-11 June 1997, Dallas, Texas.
7. Barroux, C.C., Duchet-Suchaux, P., Samier P., and Nabil, R. 2000. Linking Reservoir and Surface Simulators: How to Improve the Coupled Solutions. Paper SPE 65159-MS presented at SPE European Petroleum Conference, 24.25 October 2000, Paris, France.
8. Trick, M.D. 1998. A Different Approach to Coupling A Reservoir Simulator With A Surface Facilities Models. Paper SPE 40001-MS presented at SPE Gas Technology Symposium, 15-18 March 1998, Calgary, Alberta, Canada.
9. Foss, B.A., and Halvorsen, I.J. 2009. Dynamic optimization of the LNG value chain. Proceedings of the 1st annual gas processing symposium Doha, Qatar.
10. Tomasgard, A., Rømo, F., Fodstad, M. and Midthun, K. 2007. Optimization Models for the Natural Gas Value Chain. In Geometric Modelling, Numerical Simulation, and Optimization, Springer pp. 521-558.
11. Killough, J.E., and Kossack, C.A. 1987. Paper SPE 16000. Fifth SPE Comparative Solution Project: Evaluation of Miscible flood Simulators.
12. Sensor Reference Manual. Coats Engineering , Inc. 2009
13. Ikoku, C.U. 1984. Natural Gas Reservoir Engineering. New York, Wiley.
14. Beggs, H.D., and Brill, J.P. 1973. A Study of Two-Phase Flow in Inclined Pipes. J. Petrol. Tech., pp. 607, May.
15. Lagarias, J.C., Reeds, J.A., Wright, M.H., and Wright, P.E. 1998. Convergence Properties of The Nelder-Mead Simplex Method in Low Dimensions. SIAM J. Optimization Vol.9 No.1 pp. 112-147.

Acknowledgements

We acknowledge our collegues Mohammad Faizul Hoda from PERA and Aleksander Juell from Norwegian University of Science and Technology (NTNU). We are grateful for the assistance from Prof. Michael Golan at NTNU, Robert Hubbard from John M. Campbell&Co and Ken Starling from Starling & Associates, for helping with the surface process development. We also acknowledge financial support by the Center for Integrated Operations in the Petroleum Industry at NTNU.

SI Metric Conversion Factors

Bbl	x	1.589873	E-01	=	m^3
ft^3	x	2.831685	E-02	=	m^3
Psi	x	6.894757	E+00	=	kPa

Table 6 – Comparison results between base case and optimization.

		Optimization	
	Base Case	Scenario 1	Scenario 2
Cumulative sales gas (m^3)	1.05E+10	1.33E+10	1.16E+10
Cumulative NGL (m^3)	5.52E+06	6.51E+06	6.36E+06
Cumulative Condensate (m^3)	3.59E+07	3.58E+07	4.30E+07
NPV (USD)	6.03E+09	6.63E+09	7.11E+09
Number of iterations	1	267	334
CPU run time (hour)	0.09	28.11	34.45

Table 7 – EOS properties for oil reservoir.

Component	M	TC	PC	ZCRIT	S	AC
		K	bara			
C1	16.04	190.56	46.04	0.29	-0.15193	0.013
C3	44.1	369.83	42.49	0.277	-0.06428	0.1524
C6	86.18	507.44	30.12	0.264	0.07822	0.3007
C10	142.29	617.67	20.96	0.257	0.16895	0.4885
C15	206	705.56	13.79	0.245	0.33057	0.65
C20	282	766.67	11.17	0.235	0.32443	0.85

Table 8 – Binary Interaction Parameters (BIP) for oil reservoir.

	C1	C3	C6	C10	C15	C20
C1	0					
C3	0	0				
C6	0	0	0			
C10	0	0	0	0		
C15	0.05	0.005	0	0	0	
C20	0.05	0.005	0	0	0	0

Table 9 – Initial composition and EOS calculated properties for oil reservoir.

Initial Composition					
C1	C3	C6	C10	C15	C20
0.5	0.03	0.07	0.2	0.15	0.05
EOS calculated properties					
Ps (bara)	GOR (m^3/m^3)	ρ_{gs} (kg/m^3)	μ_{gs} (cp)	ρ_{os} (kg/m^3)	μ_{os} (cp)
158.8	104.3	111.5	0.017	540.9	0.2

Table 10 – Production and injection wells location.

Well	Reservoir								
	Lean Gas-Condensate			Rich Gas-Condensate			Oil		
	i	j	k	i	j	k	i	j	k
PROD 1	25	25	1 - 4	25	25	1 - 4	21	21	1 - 3
PROD 2	14	13	1 - 4	14	13	1 - 4	10	9	1 - 3
PROD 3	32	5	1 - 4	32	5	1 - 4	32	5	1- 3
PROD 4	15	31	1 - 4	15	31	1 - 4	13	29	1 - 3
PROD 5	6	23	1 - 4	6	23	1 - 4	8	21	1 - 3
GINJ 1	19	19	1 - 4	19	19	1 - 4	15	15	1 - 3
GINJ 2	9	6	1 - 4	9	6	1 - 4	5	5	1 - 3
GINJ 3	32	32	1 - 4	32	32	1 - 4	28	27	1 - 3
GINJ 4	30	9	1 - 4	30	9	1 - 4	29	11	1 - 3
GINJ 5	14	23	1 - 4	14	23	1 - 4	14	23	1 - 3
GINJ 6	5	32	1 - 4	5	32	1 - 4	5	32	1 - 3
GINJ 7	22	34	1 - 4	22	34	1 - 4	22	34	1 - 3
GINJ 8	3	16	1 - 4	3	16	1 - 4	3	16	1 - 3

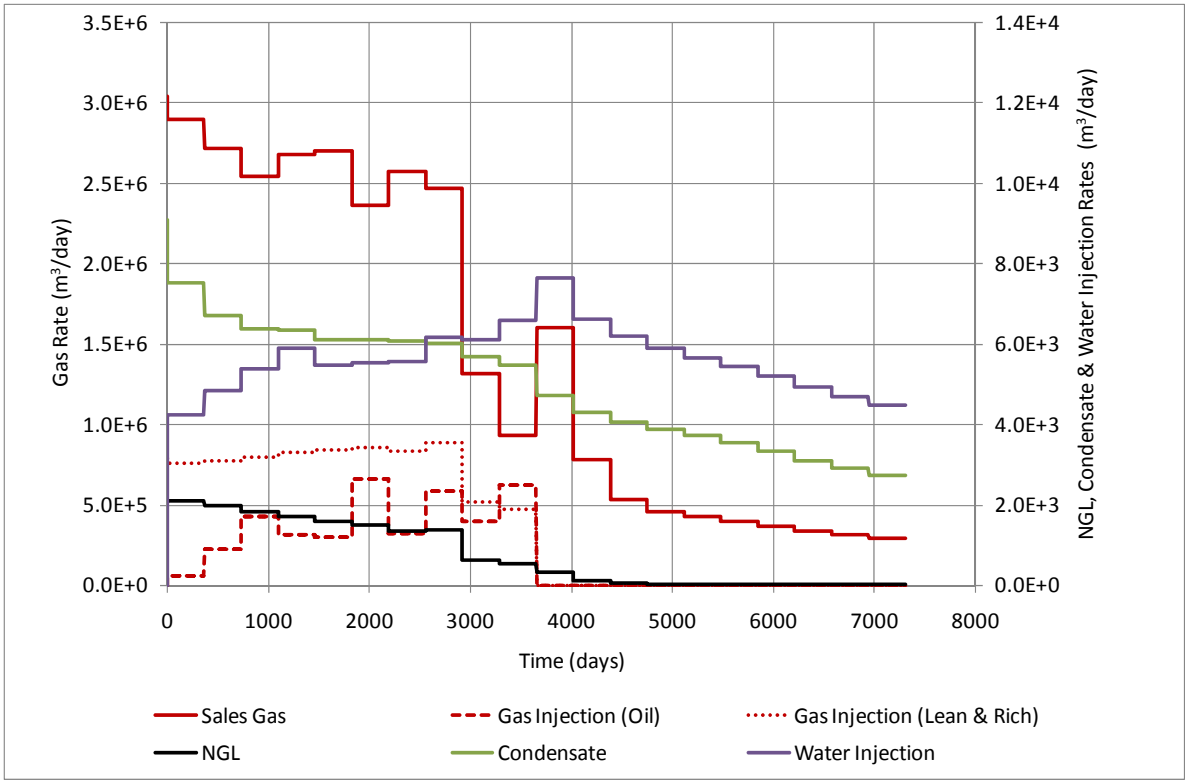

Fig. 6 – Sales products and injection rates for the base case.

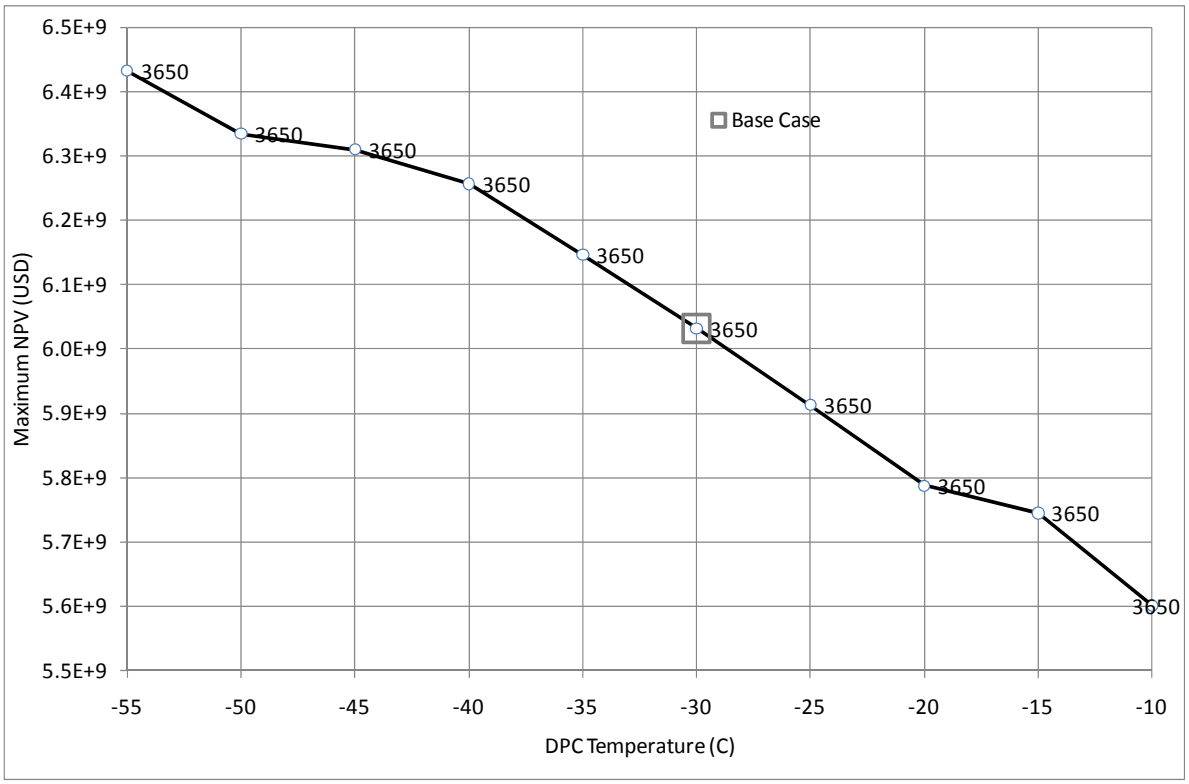

Fig. 7 – Single parameter analysis for DPC temperature. The lowest temperature gives the highest NPV.

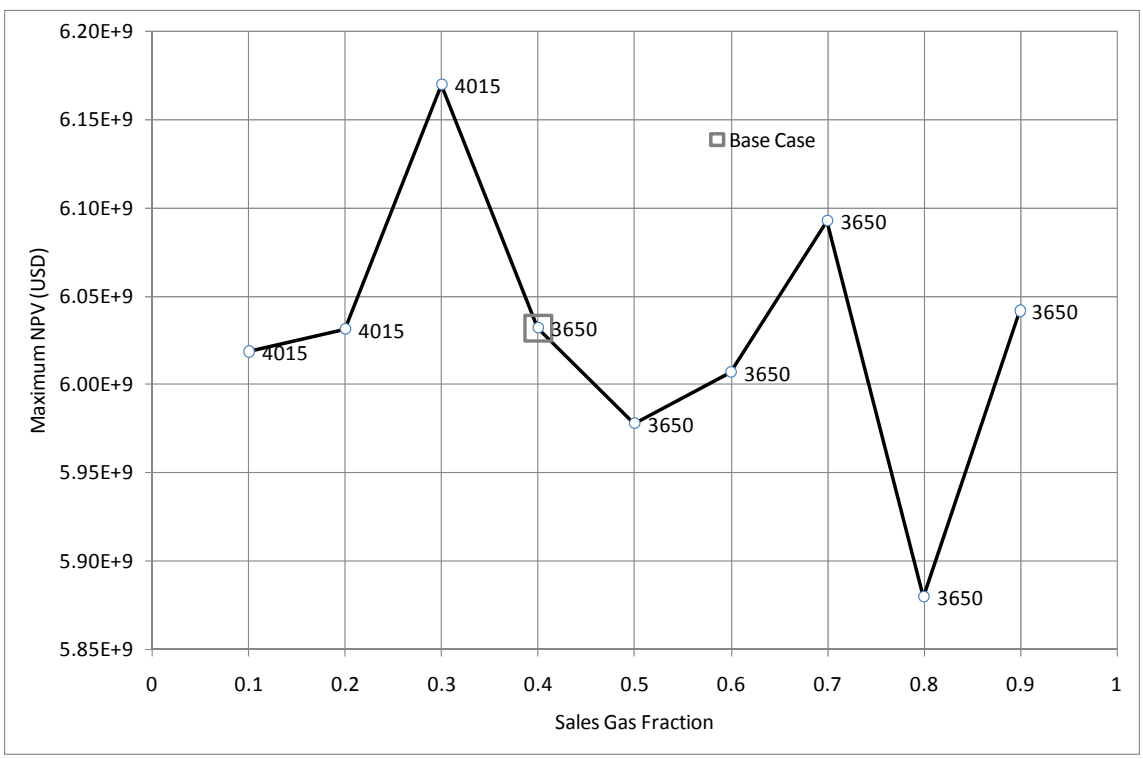

Fig. 8 – Single parameter analysis for sales gas fraction. The maximum NPV is obtained at $f_{sg} = 0.3$.

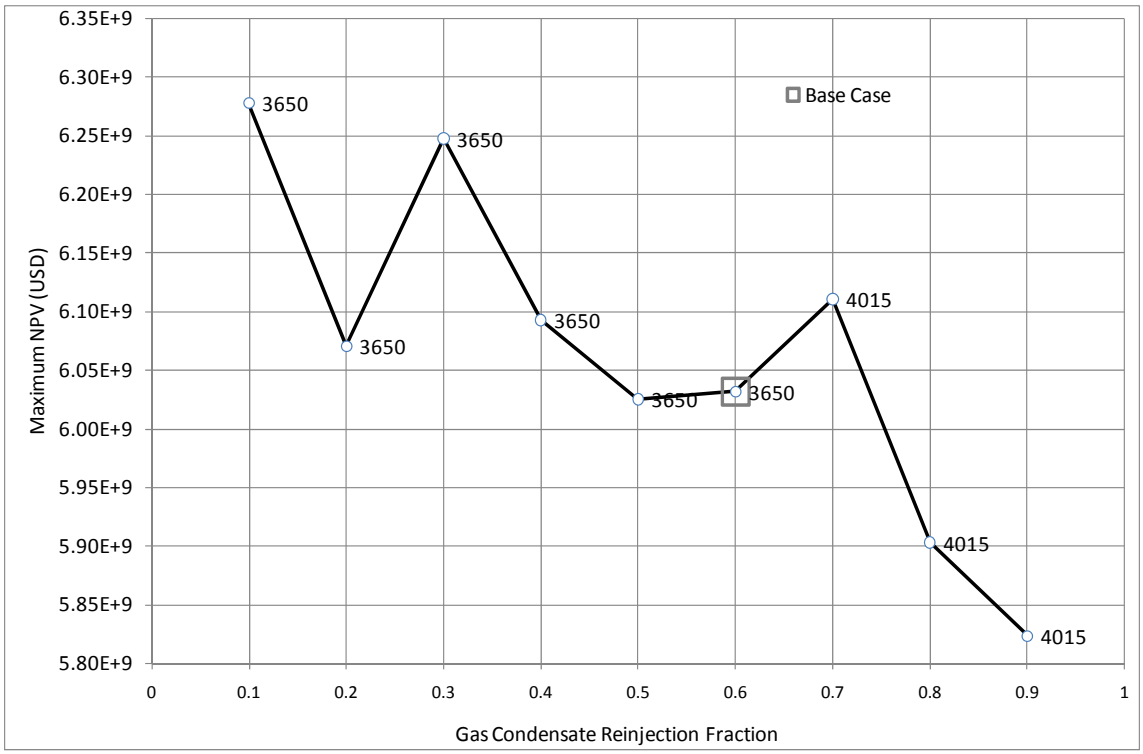

Fig. 9 – Single parameter analysis for gas-condensate reinjection fraction. The maximum NPV is obtained at $f_{R_{gc}} = 0.1$.

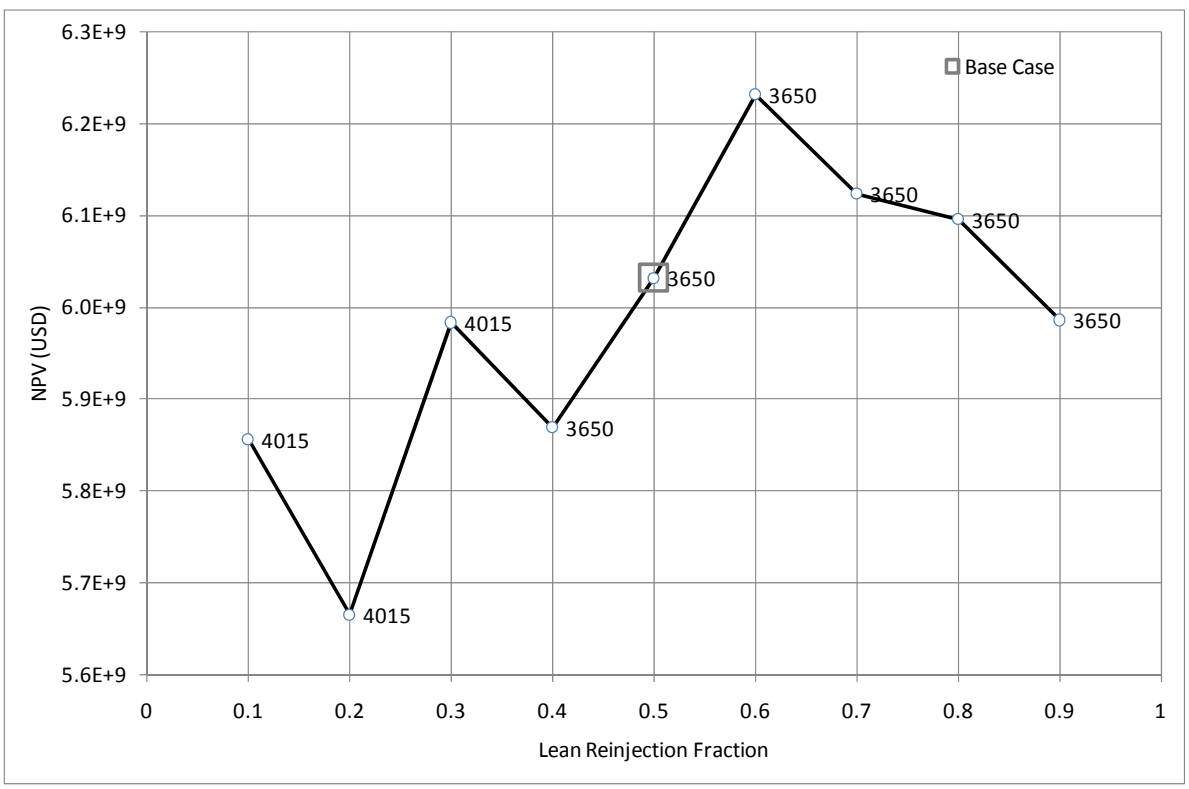

Fig. 10 – Single parameter analysis for lean reinjection fraction. The maximum NPV is obtained at $f_{R_L} = 0.6$.

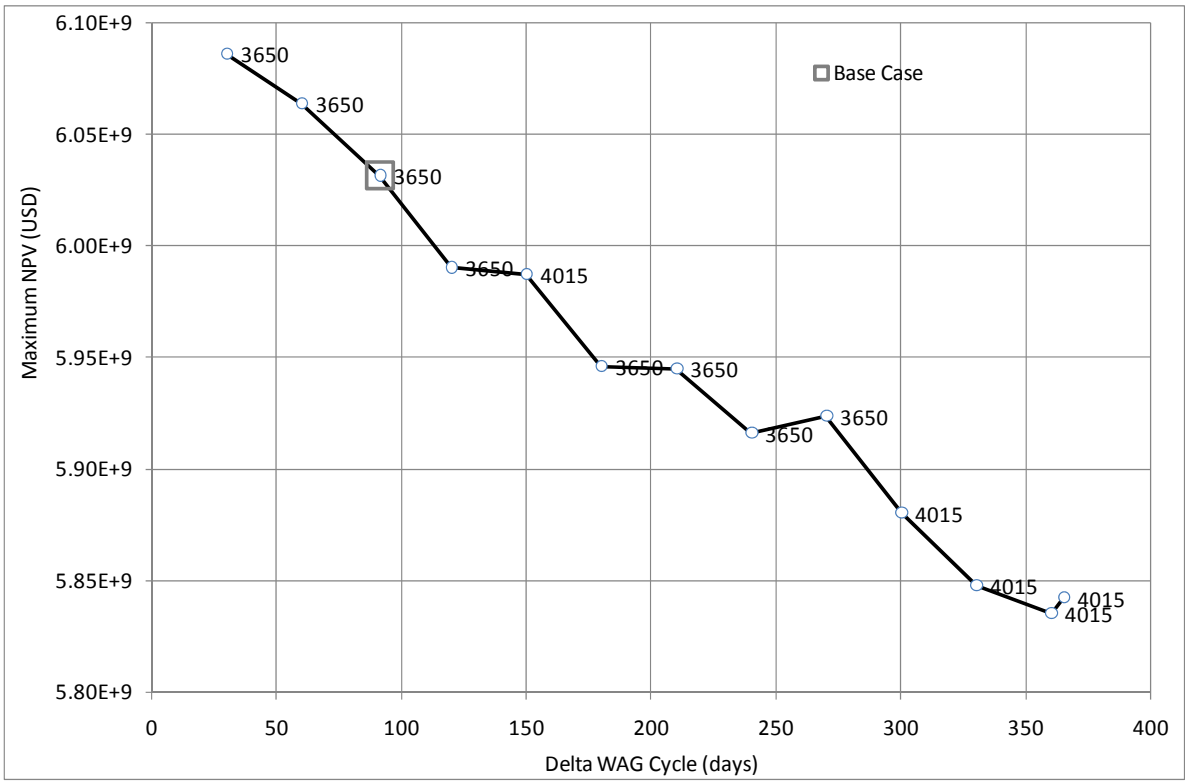

Fig. 11 – Single parameter analysis for the WAG cycle time.
This figure indicates that the best scenario for the oil reservoir is implementing Simultaneous WAG (SWAG).

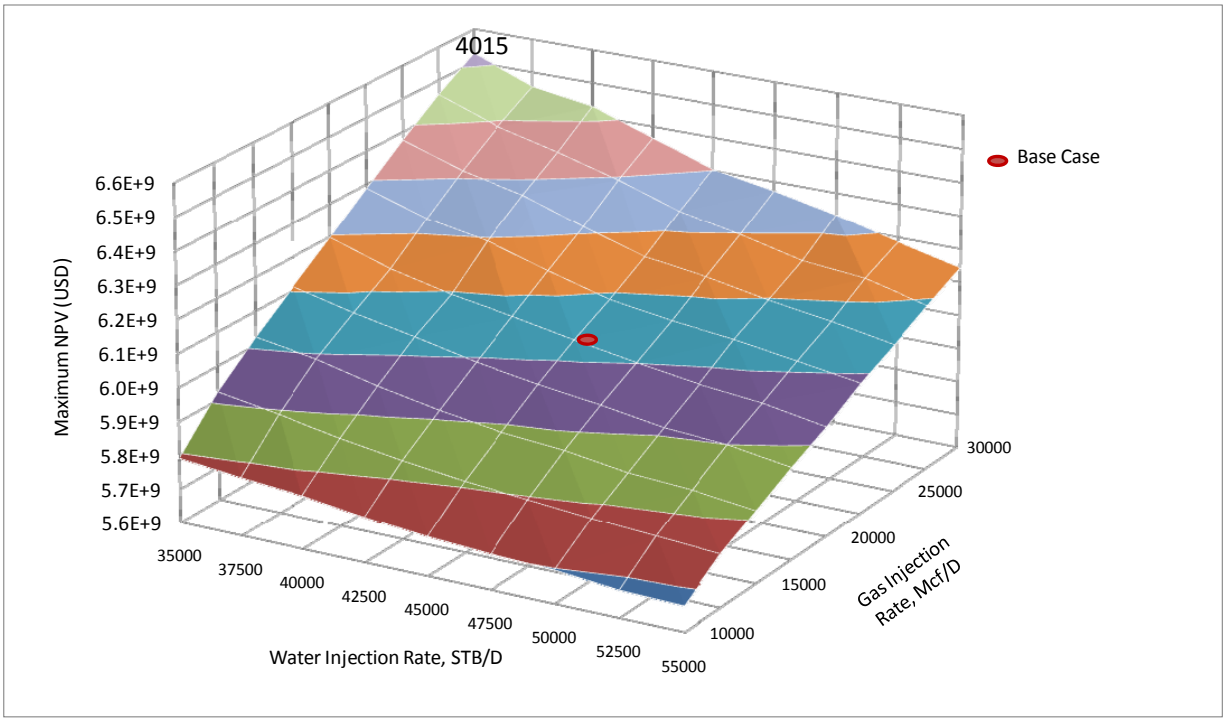

Fig. 12 – Surface parameter analysis for water and gas injection rates for WAG scenario.
This figure shows that the maximum NPV is obtained for high gas injection rate and a low water injection rate.

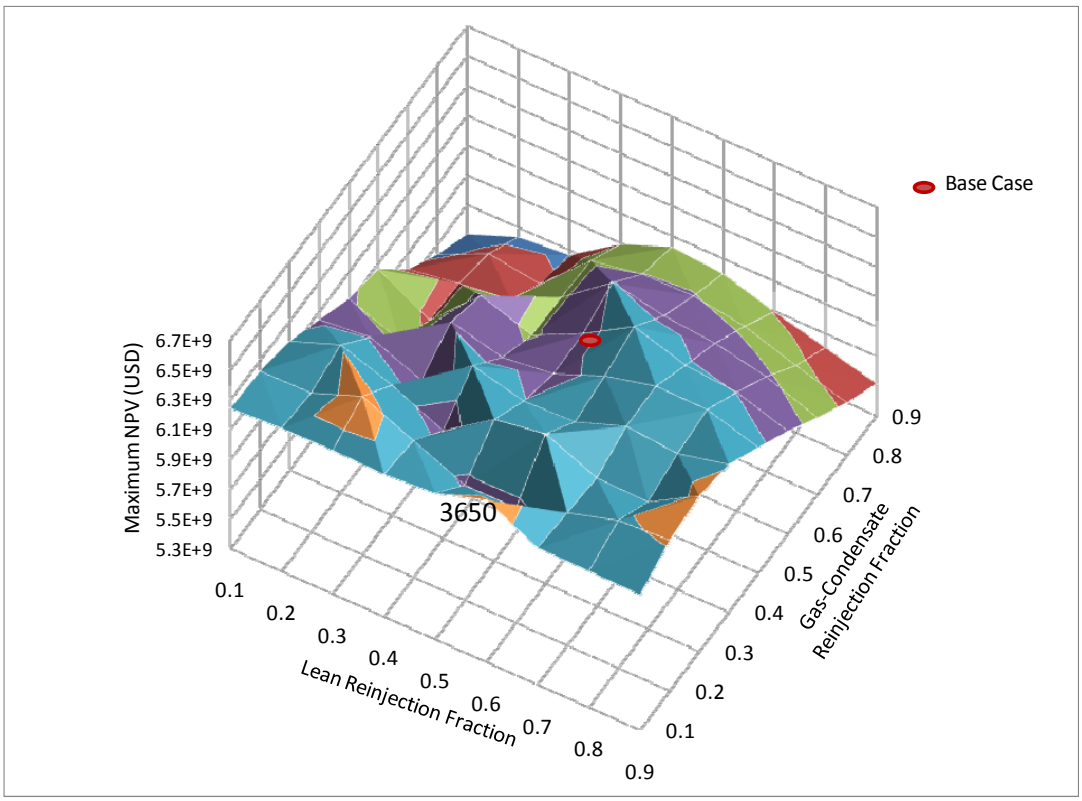

Fig. 13 – Surface parameter analysis for gas-condensate reinjection fraction and lean reinjection fraction. The maximum NPV is obtained for $f_{R_{gc}} = 0.1$ and $f_{R_L} = 0.6$.

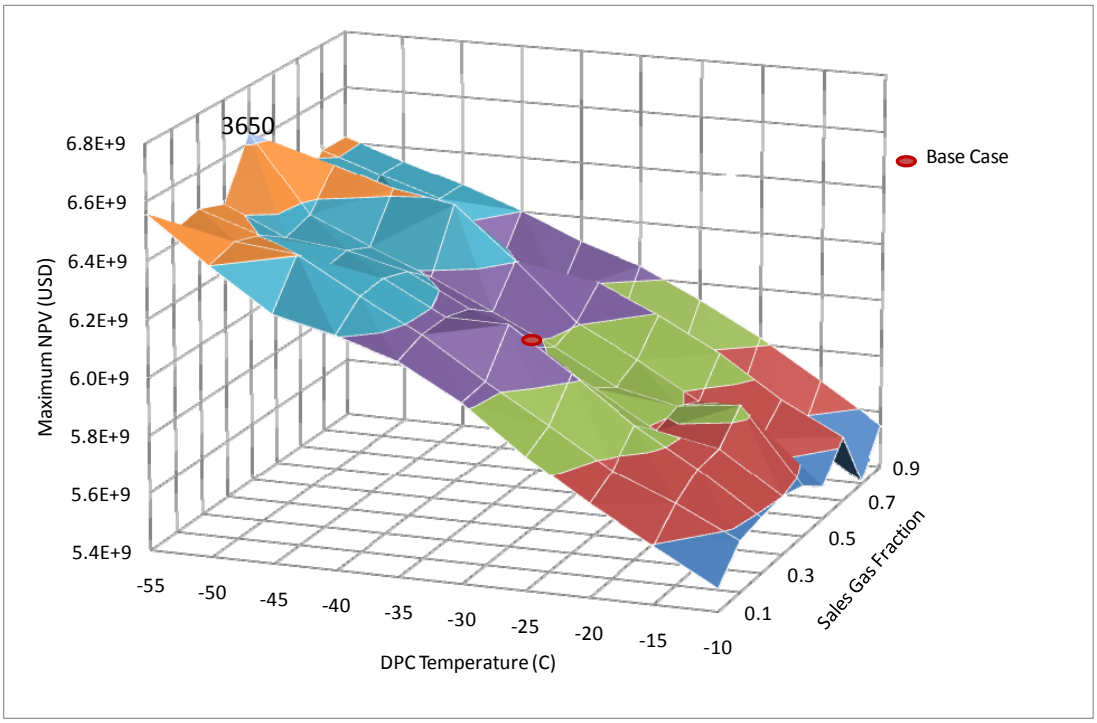

Fig. 14 – Surface parameter analysis for DPC temperature and sales gas fraction. The maximum NPV is obtained when $f_{sg} = 0.5$ and $T_{DPC} = -55^{\circ}$C.

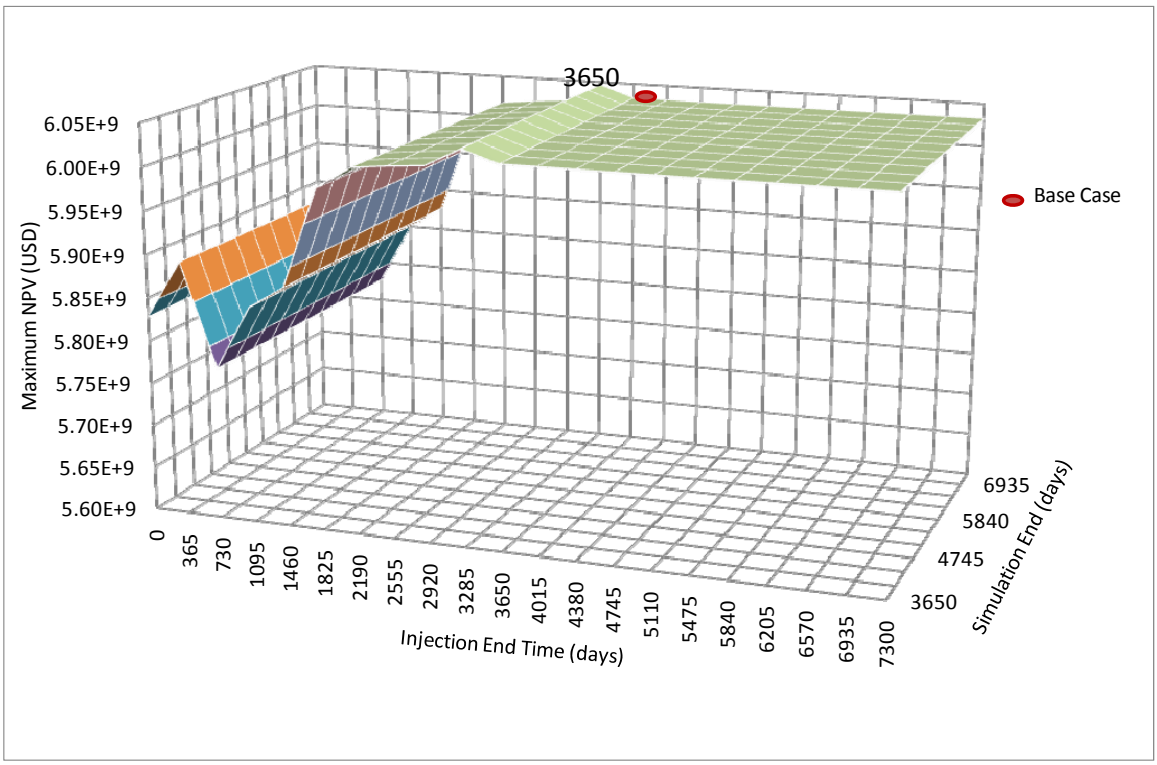

Fig. 15 – Surface parameter analysis for varying injection end time and simulation end time.

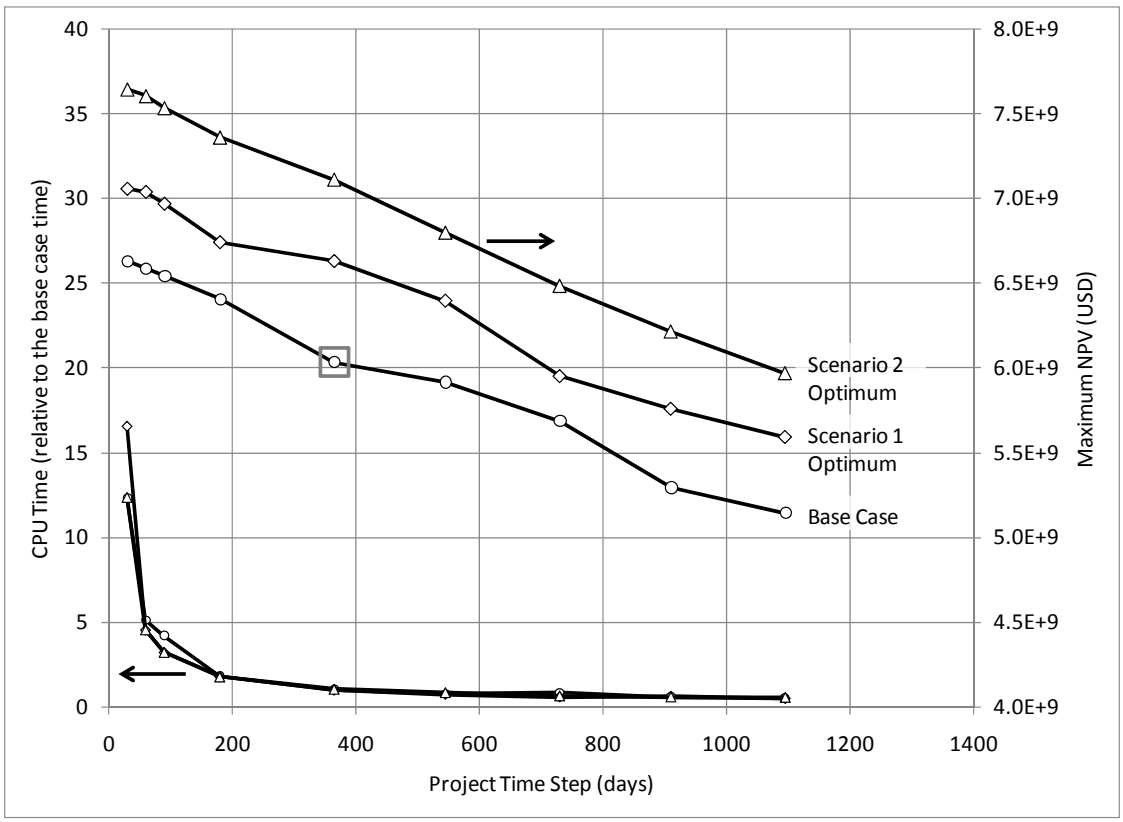

Fig. 16 – NPV for different project time steps.